AMERICAN SOCIETY FOR MICROBIOLOGY | Molecular and Cellular Biology

Mechanisms Underlying Acrolein-Mediated Inhibition of Chromatin Assembly

Lei Fang,[a,b] Danqi Chen,[a] Clinton Yu,[c] Hongjie Li,[a,d] Jason Brocato,[a] Lan Huang,[c] Chunyuan Jin[a]

Department of Environmental Medicine & Biochemistry and Molecular Pharmacology, New York University School of Medicine, Tuxedo, New York, USA[a]; Medical School of Nanjing University, Nanjing, China[b]; Department of Physiology & Biophysics, University of California, Irvine, California, USA[c]; Department of Pathology, SUNY Downstate Medical Center, New York, New York, USA[d]

Acrolein is a major component of cigarette smoke and cooking fumes. Previously, we reported that acrolein compromises chromatin assembly; however, underlying mechanisms have not been defined. Here, we report that acrolein reacts with lysine residues, including lysines 5 and 12, sites important for chromatin assembly, on histone H4 *in vitro* and *in vivo*. Acrolein-modified histones are resistant to acetylation, suggesting that the reduced H4K12 acetylation that occurs following acrolein exposure is probably due to the formation of acrolein-histone lysine adducts. Accordingly, the association of H3/H4 with the histone chaperone ASF1 and importin 4 is disrupted and the translocation of green fluorescent protein-tagged H3 is inhibited in cells exposed to acrolein. Interestingly, *in vitro* plasmid supercoiling assays revealed that treatment of either histones or ASF1 with acrolein has no effect on the formation of plasmid supercoiling, indicating that acrolein-protein adduct formation itself does not directly interfere with nucleosome assembly. Notably, exposure of histones to acrolein prior to histone acetylation leads to the inhibition of remodeling and spacing factor chromatin assembly, which requires acetylated histones for efficient assembly. These results suggest that acrolein compromises chromatin assembly by reacting with histone lysine residues at the sites critical for chromatin assembly and prevents these sites from physiological modifications.

Acrolein (Acr) is an α,β-unsaturated aldehyde that ubiquitously exists in cigarette smoke, kitchen cooking oil, and exhaust of automobiles (1–3). Acr has been implicated in the development of multiple human diseases, such as bladder cancer (4), lung cancer (5–7), Alzheimer's disease (8–10), and cardiovascular diseases (11, 12). Acr contains a carbonyl group and an olefinic double bond, which makes it highly reactive to many cellular molecules, including proteins and DNA (13–16). Recent studies show that Acr could be a potential major carcinogen of smoking-related lung cancer via induction of DNA damage and inhibition of DNA repair (14, 15, 17, 18). In addition to its role in inducing DNA damage and mutagenicity, the other biological effects of Acr are most likely through its direct interaction with nucleophilic amino acids, primarily cysteine, lysine, and histidine, in critical protein targets (11, 12, 19). These proteins include transcription activation factor NF-κB (20, 21), caspases that regulate cell apoptosis (7, 22), and proteins involved in redox signaling regulation (16, 19). As a highly reactive chemical, in theory, Acr could react with a large number of other proteins and affect their functions. However, the molecular consequences of the formation of Acr-protein adducts remain unclear.

In a previous study, we found that Acr interacts with histone proteins to form Acr adducts (23). Moreover, Acr exposure dramatically downregulates critical posttranslational modifications on newly synthesized histones, such as H4K12ac and H3K9&K14ac, and compromises chromatin assembly (23). Recent studies have provided insight into the roles of histone modifications and histone chaperones in regulating chromatin assembly (24–27). Histone modifications affect chromatin assembly in various ways, including the regulation of histone folding and processing, histone nuclear import, and the interaction between histones and histone chaperones (28–31). For example, H4K5&K12ac, a diacetylation catalyzed by histone acetyltransferase 1(HAT1)-RbAp46, is detected on newly synthesized histone H4 from yeast to humans as an early modification occurring on H3-H4 (32–36). The H4K5&K12 double mutants are imported into the nucleus less efficiently than wild-type histones (32, 37). Moreover, HAT1-RbAp46 and H4K5&K12 regulate the association of H3-H4 with the translocator protein importin 4 and the histone chaperone ASF1 (31, 32, 36, 37). These results indicate that H4K5&K12 might regulate chromatin assembly pathways by regulating H3-H4 nuclear import. Other histone acetylations, such as H4K79ac and H4K91ac (38), H3K9ac and H3K27ac (39), and H3K56ac (40–43), have also been reported to play roles in chromatin assembly, probably by regulating the interaction between histones and histone chaperones. The reduction of H4K12ac that we previously observed in cells exposed to Acr might be due to the reaction of Acr with H4K12. However, we have not determined if Acr targets H4K12 and other lysines important for chromatin assembly and, if so, how they affect physiological modifications at the same sites. Moreover, it is also not known whether Acr directly targets HAT and interferes with its enzyme activity, leading to the reduction of histone acetylations.

Histone chaperones bind to histones and regulate histone transfer, transport, or storage, thereby modulating chromatin assembly (24, 26, 27, 36). Newly synthesized H3-H4 molecules associate with HAT1, which acetylates H4K5&K12 (31, 32, 34, 35, 44). After acetylation, the histones are bound to ASF1,

Received 3 August 2016 **Accepted** 14 September 2016

Accepted manuscript posted online 26 September 2016

Citation Fang L, Chen D, Yu C, Li H, Brocato J, Huang L, Jin C. 2016. Mechanisms underlying acrolein-mediated inhibition of chromatin assembly. Mol Cell Biol 36:2995–3008. doi:10.1128/MCB.00448-16.

Address correspondence to Chunyuan Jin, Chunyuan.jin@nyumc.org.

which associates with importin 4. Thus, downregulation of H4K12ac may disrupt the association of H3/H4 with ASF1 and importin 4, inhibiting histone nuclear translocation (28, 45, 46). After nuclear import, the H3-H4 dimer of the ASF1 complex is transferred to the central histone chaperone CAF-1, which binds two H3-H4 dimers to form $(H3\text{-}H4)_2$ tetramers and deposits them onto replicating DNA through the CAF-1–proliferating cell nuclear antigen interaction (47, 48). Independently of Acr-induced downregulation of histone modifications, the formation of Acr adducts with histone chaperones may directly affect both the interaction between histones and histone chaperones and the nucleosome assembly activity of histone chaperones.

In this study, we used mass spectrometry and several biochemistry approaches to explore the molecular mechanism whereby Acr compromises chromatin assembly. We found that the formation of Acr-histone lysine adducts is probably the main contributor of Acr-induced reduction of histone acetylation at the sites important for histone-protein interactions. Accordingly, the association of H3/H4 with ASF1 and importin 4 is disrupted in cells following Acr exposure. Furthermore, the exposure of histones to Acr *in vitro* prevents histone acetylation by the CREB-binding protein (CBP) HAT and inhibits RSF (remodeling and spacing factor)-mediated chromatin assembly, which requires acetylated histones for efficient assembly. Interestingly, Acr modification itself, either on histones or on ASF1, has little or no effect on protein-protein interaction and plasmid supercoiling *in vitro*. Taken together, our data identify the molecular mechanisms underlying Acr-induced inhibition of chromatin assembly and suggests that prevention of physiological modifications at critical sites might be a novel mechanism whereby Acr-protein adducts perturb protein functions.

MATERIALS AND METHODS

Cells and plasmids. Plasmid pcDNA3.1-FLAG-H3.1 was constructed in our previous study (49). This plasmid was transfected into BEAS-2B cells with Lipofectamine 2000 (Invitrogen) and selected with hygromycin (500 μg/ml) to generate a BEAS-2B-FLAG-H3.1 stable cell line. A cDNA fragment of H3.1 was amplified by PCR with pcDNA3.1-FLAG-H3.1 as a template. Forward primer 5′-CAGATCTATGGCTCGTACGAAGCA AAC-3′ and reverse primer 5′-ATCTAGACTAGGCGTAGTCGGGC ACG-3′ were used. The fragment was cloned into the BglII/XbaI sites of puHD-EGFP to generate the puHD-EGFP-H3.1 construct. The plasmid was transfected into UTA6 human osteosarcoma cells, which contain tetracycline transactivator tTA, with Lipofectamine 2000 (Invitrogen) and selected with zeocin (60 μg/ml) to generate an inducible UTA6-EGFP-H3.1 stable cell line.

The immortalized human bronchial epithelial cell line BEAS-2B, the BEAS-2B-FLAG-H3.1 stable cell line, and the UTA6-EGFP-H3.1 stable cell line were cultured in Dulbecco's modified Eagle's medium (DMEM) supplemented with 10% fetal bovine serum. Cells were grown overnight to ~70 to 80% confluence and exposed to Acr as previously described (23). A glutathione *S*-transferase (GST)–CBP plasmid was kindly provided by Kazunari Yokoyama. A BS II plasmid was obtained from Addgene. FLAG-tagged Rsf-1 and hSNF2H baculoviruses for RSF purification and a GST-ASF1B construct were generously provided by Danny Reinberg.

Antibodies. Anti-FDP-K (ab48501), anti-histone H3 (ab1791), anti-acetyl-histone H4 Lys5 (ab124636), anti-acetyl-histone H4 Lys12 (ab61238), and anti-γ-tubulin (ab11317) antibodies were purchased from Abcam; anti-HAT1 (sc376200), anti-importin 4 (sc292402), and anti-ASF1B (sc79849) antibodies were purchased from Santa Cruz Biotechnology; an anti-FLAG antibody (F3165) was purchased from Sigma; and an anti-GST antibody (MA4-004) was purchased from Pierce.

Cell fractionation, Co-IP, and Western blot analysis. BEAS-2B cells that stably expressed FLAG-tagged histone H3.1 treated or not treated with Acr (4×10^7) were suspended in 1.5 ml of hypotonic buffer (10 mM Tris-HCl [pH 7.4], 10 mM KCl, 1.5 mM $MgCl_2$, 1 mM dithiothreitol [DTT], protease inhibitors) for 10 min on ice and centrifuged at 2,500 × *g* for 10 min after being passed four times through a 25-gauge needle to obtain the cytosolic fraction. The supernatant was collected and further ultracentrifuged at 25,000 rpm for 30 min before coimmunoprecipitation (Co-IP). Immunoprecipitation (IP) and Western blot analysis were carried out as described elsewhere (23).

Identification of histone modifications by LC-MS/MS and database searching. Recombinant histones H2A and H4 were treated with 50 μM Acr at 37°C overnight. For identification of histone modifications by Acr *in vivo*, IP with FDP-K antibody was performed to enrich Acr-modified histones from BEAS-2B cells exposed to 100 μM Acr for 2 h. The resulting Acr-modified proteins were separated by SDS-PAGE, digested in gel with the desired enzymes, and analyzed by liquid chromatography-tandem mass spectrometry (LC-MS/MS) as described previously (50, 51). Briefly, LC-MS/MS was carried out with an LTQ-Orbitrap XL mass spectrometer (Thermo Scientific, San Jose, CA) coupled online with an EASY-nLC-1000 (Thermo Scientific, San Jose, CA). For MS/MS analysis of peptides, a cycle of one full Fourier transform scan (350 to 1,400 *m*/*z*, resolution of 60,000 at *m*/*z* 400) was followed by 10 cycles of data-dependent MS/MS acquired in the LTQ with normalized collision energy set at 35%. MS/MS data were extracted and searched against a decoy database consisting of a normal SwissProt database concatenated with its randomized version (SwissProt.2013.6.17.random.concat with a total of 455,294 protein entries) with a developmental version of Protein Prospector (v5.10.10; University of California, San Francisco). *Homo sapiens* was set as the species (20,501 entries) for analysis of data. The mass tolerances for parent and fragment ions were set as ±20 ppm and ±0.6 Da, respectively. For trypsin digestion, trypsin was set as the enzyme with five maximum missed cleavages allowed. Protein N-terminal and lysine acetylation, cysteine carbamidomethylation, asparagine deamidation, N-terminal conversion of glutamine to pyroglutamic acid, methionine oxidation, lysine methylation, lysine and arginine dimethylation, lysine trimethylation, aldimine-modified arginine, aldimine-modified lysine, *N*(ε)-3-formyl-3,4-dehydropiperidino (FDP)-modified lysine, *N*(ε)-3-methylpyridinium (MP)-modified lysine, propanal-modified histidine, and glygly-modified lysine were selected as variable modifications. The expectation value threshold was set at ≥0.05 for peptide identification.

HAT assays. EpiQuick HAT activity/inhibition assays were performed in accordance with the manual instructions, with slight modification. HT2 histone peptides were left untreated or treated with 100 μM Acr, incubated overnight at 37°C, and then used as substrates for HAT activity assays. The cytosolic fractions isolated from BEAS-2B cells were used as sources of HAT enzyme.

For CBP HAT assays, 1 μg of recombinant H3.1 or H4 was treated with 0, 25, 50, or 100 μM Acr in 1× phosphate-buffered saline (PBS) overnight at 37°C and then incubated with 0.1 μg of GST-CBP prepared from *Escherichia coli* and acetyl coenzyme A (acetyl-CoA) in 1× HAT buffer (50 mM Tris-Cl [pH 8.0], 10% glycerol, 0.1 mM EDTA, 1 mM DTT) for 1 h at 37°C. In the other case, 0.1 μg of GST-CBP proteins was treated with 0, 25, 50, or 100 μM Acr in 1× PBS overnight at 37°C, followed by removal of Acr by dialysis, and then incubated with 1 μg of recombinant H4 and acetyl-CoA in 1× HAT buffer for 1 h at 37°C. The acetylation of H3.1 or H4 was analyzed by Western blotting with antibody to H3K9&K14ac or H4K12ac, respectively. The same samples were also probed with the anti-FDP-K antibody to monitor histone-Acr adduct formation.

HAT assays of FLAG-HAT1 were carried out similarly by replacing GST-CBP with FLAG-HAT1.

Purification of H3.1-H4 tetramer and GST pulldown assay. Recombinant *Xenopus* histones H3, H2A, H2B, and H4 were expressed and pu-

rified separately from *E. coli* as described by K. Luger et al. (52, 53). Refolding of histone tetramers was performed essentially as described previously (52, 53), with recombinant histones H3.1 and H4. The refolded H3.1-H4 mixture was loaded onto a HiLoad 16/600 Superdex 200 gel filtration column (GE Healthcare). Gel filtration fractions were collected and analyzed by both measurement of optical density at 276 nm and Coomassie blue staining. The fractions from 70 to 79 ml, which contained H3.1-H4 tetramers, were pooled and concentrated. GST-ASF1B protein was expressed in and purified from *E. coli* as previously described (54). For GST pulldown assays, 5 μg of H3.1-H4 tetramers was treated with 0, 25, 50, or 100 μM Acr in 1× PBS and then mixed with 5 μg of GST-ASF1B. In some cases, 5 μg of GST-ASF1B was first treated with 0, 25, 50, or 100 μM Acr and then mixed with 5 μg of H3.1-H4 tetramers. The reaction mixture was incubated with shaking for 30 min at 4°C in binding buffer (20 mM Tris-HCl [pH 7.5], 200 mM NaCl, 0.1% [wt/vol] bovine serum albumin [BSA], 5 mM 2-mercaptoethanol, 0.01% IGEPAL CA-630, 10% glycerol). Ten microliters of glutathione-agarose was then added, and the mixture was rotated for 30 min. The resin was washed three times with 1 ml of W500 (20 mM Tris-HCl [pH 7.5], 500 mM NaCl, 0.1% [wt/vol] BSA, 5 mM 2-mercaptoethanol, 0.1% IGEPAL CA-630, 10% glycerol) and three times with 1 ml of W200 and eluted with boiling resin in 1× SDS-PAGE sample buffer.

Time-lapse fluorescence microscopy analysis. UTA6-EGFP-H3 stable cells were generated and maintained in DMEM supplemented with tetracycline and zeocin. Expression of enhanced green fluorescent protein (EGFP)-tagged H3 was induced by removal of tetracycline and overnight growth in normal DMEM. The cells were treated with 20 μM MG132 for 2 h and then treated with 100 μM Acr for an additional 2 h or not treated with Acr. Images were captured every 2 min.

Plasmid supercoiling assay. A plasmid supercoiling assay was performed as described elsewhere (30, 55). Either core histones or GST-ASF1B was treated with 0, 25, or 50 μM Acr in 1× PBS overnight at 37°C. A 0.09-μg sample of core histones was mixed with 0.8 μg of GST-ASF1B. The mixture was then incubated with 0.1 μg of BS II plasmid relaxed with topoisomerase I (Promega) to introduce plasmid supercoiling. The DNA was extracted and analyzed by electrophoresis on a 1.2% agarose gel and then ethidium bromide stained.

RSF-mediated chromatin assembly. Recombinant RSF purification and RSF-mediated chromatin assembly were performed as described by Loyola et al. (56). Briefly, 100 μg of histone octamers was first dialyzed in low-salt buffer (10 mM Tris-HCl [pH 7.5], 100 mM NaCl) to generate mostly H2A-H2B dimers and H3.1-H4 tetramers and then treated with 0 or 100 μM Acr at 37°C overnight. A 1.8-μg sample of an H2A-H2B dimer and H3.1-H4 tetramer mixture was then incubated with GST-CBP and acetyl-CoA at 37°C for 1 h in 1× HAT buffer (50 mM Tris-Cl [pH 8.0], 10% glycerol, 0.1 mM EDTA, 1 mM DTT) to produce acetylated histones, including H2A/H2B. The core histone mixture was further incubated with 2 μg of BS II plasmid in the presence of 0.3 μg of recombinant RSF, 150 μg of BSA, 3 mM ATP, 30 mM phosphocreatine (Sigma), 0.2 μg of phosphocreatine kinase (Sigma), 5 mM $MgCl_2$, 50 mM KCl, 10 mM Tris-Cl (pH 7.6), 0.2 mM EDTA, and 5% glycerol in a final reaction volume of 150 μl. The reaction mixture was incubated at 30°C overnight and then subjected to partial micrococcal nuclease (MNase) digestion to assess the formation of regular nucleosomal arrays. The MNase concentration was optimized (192 U/ml) to obtain clear nucleosome arrays. DNA was extracted and analyzed by electrophoresis on a 1.5% agarose gel.

Statistical analysis. Gel staining and Western blot intensities were quantified with ImageJ processing software (National Institutes of Health). Relevant results are represented as mean values ± standard deviations (SD; error bars). Significance was assessed by Student's *t* test. A *P* value of <0.05 was considered statistically significant. The number of times each experiment was repeated is indicated in the figure legends.

RESULTS

Identification of the sites of Acr-lysine adducts on recombinant histones H2A and H4 following Acr exposure by mass spectrometry. We previously reported the formation of Acr-lysine adducts on histones with antibodies that recognize Acr-lysine adducts (23). However, it has not been determined which lysines are targeted by Acr. We used LC-MS/MS to define the sites of Acr-lysine adducts on recombinant histones H2A and H4 exposed to Acr. Peptide sequencing by MS/MS allows unambiguous identification of modified histone peptides. Aldimine-lysine, MP-lysine, and FDP-lysine are three major adducts that Acr forms with lysine residues, causing mass additions of 38, 76, and 94 Da, respectively (Fig. 1A). Figure 1B displays a representative MS/MS spectrum of an Acr-modified peptide (*m/z* 674.8593^{2+}) from H2A. As shown in Fig. 1B, the observation of a series of y (y_2, y_3, $y_5{\sim}y_9$) and b (b_3, b_4, $b_7{\sim}b_{10}$) ions identified this peptide with the sequence $_{90}$NDE ELNK(MP)LLGK$_{100}$, in which K96 has a mass addition of 76 Da, corresponding to MP-modified lysine. To further confirm this sequence, we have compared its MS/MS spectrum with that of the corresponding unmodified H2A peptide (*m/z* 636.8433^{2+}) (Fig. 1C). When comparing the modified and unmodified forms, any fragment ions containing K96(MP) would have a defined mass difference (+76 Da). As expected, while b_3, b_4, y_2, and y_3 have the same masses in both spectra (Fig. 1B and C), $y_5{\sim}y_9$ and $b_7{\sim}b_{10}$ represent the changes correlating with the modification identified. Together, these results unambiguously identified the Acr-modified peptide of H2A.

Similarly, Fig. 1D displays a representative MS/MS spectrum of an Acr-modified peptide (*m/z* 710.4024^{2+}) from H4 treated with Acr. On the basis of the series of y ($y_4{\sim}y_9$, y_{11}) and b (b_2, b_3, $b_5{\sim}b_7$, b_9, b_{11}) ions observed, the peptide sequence was identified as $_{25}$DNIQGITK(FDP)PAIR$_{36}$, in which K32 has a mass addition of 94 Da, corresponding to an FDP-modified lysine. In comparison with its unmodified H4 peptide (*m/z* 663.3823^{2+}) (Fig. 1E), the molecular masses of the ions containing K32 (i.e., $y_5{\sim}y_9$, y_{11}, b_8, b_9, and b_{11}) in Fig. 1D are indeed 94 Da higher than those of the corresponding unmodified forms in Fig. 1E, further confirming the identification of FDP modification of K32.

In total, we have identified 13 Acr-modified peptides from H4 and 3 Acr-modified peptides from H2A (Table 1). In our previous study, we observed remarkable reduction of cytosolic H4K12 acetylation in cells exposed to Acr and hypothesized that Acr-lysine adducts are attributable to the reduction (23). In agreement with this prediction, we identified the Acr-modified H4K12 peptide $_9$GLGK(MP)GGAK$_{16}$ (*m/z* 382.227^{2+}) in Acr-treated recombinant H4 (Table 1). H4K5,12 acetylations regulate histone nuclear import and chromatin assembly (32). Notably, we also detected the Acr-modified H4K5 peptide $_4$GK(MP)GGKGLGK$_{12}$ (*m/z* 439.2626^{2+}), suggesting that H4K5ac could be downregulated by Acr along with H4K12ac in Acr-exposed cells. These data provide strong evidence that Acr might inhibit the acetylation of newly synthesized histones by forming Acr-lysine adducts. Interestingly, we also found that despite the high coverage of H2A and H4 in trypsin-digested samples, not all lysine residues formed adducts with Acr (Table 1), indicating specificity of Acr reactions with lysine residues by an unknown mechanism.

Identification of the sites of Acr-lysine adducts on histone H4 in cells exposed to Acr by mass spectrometry. Several Acr-modified histone lysine sites were detected by mass spectrometry

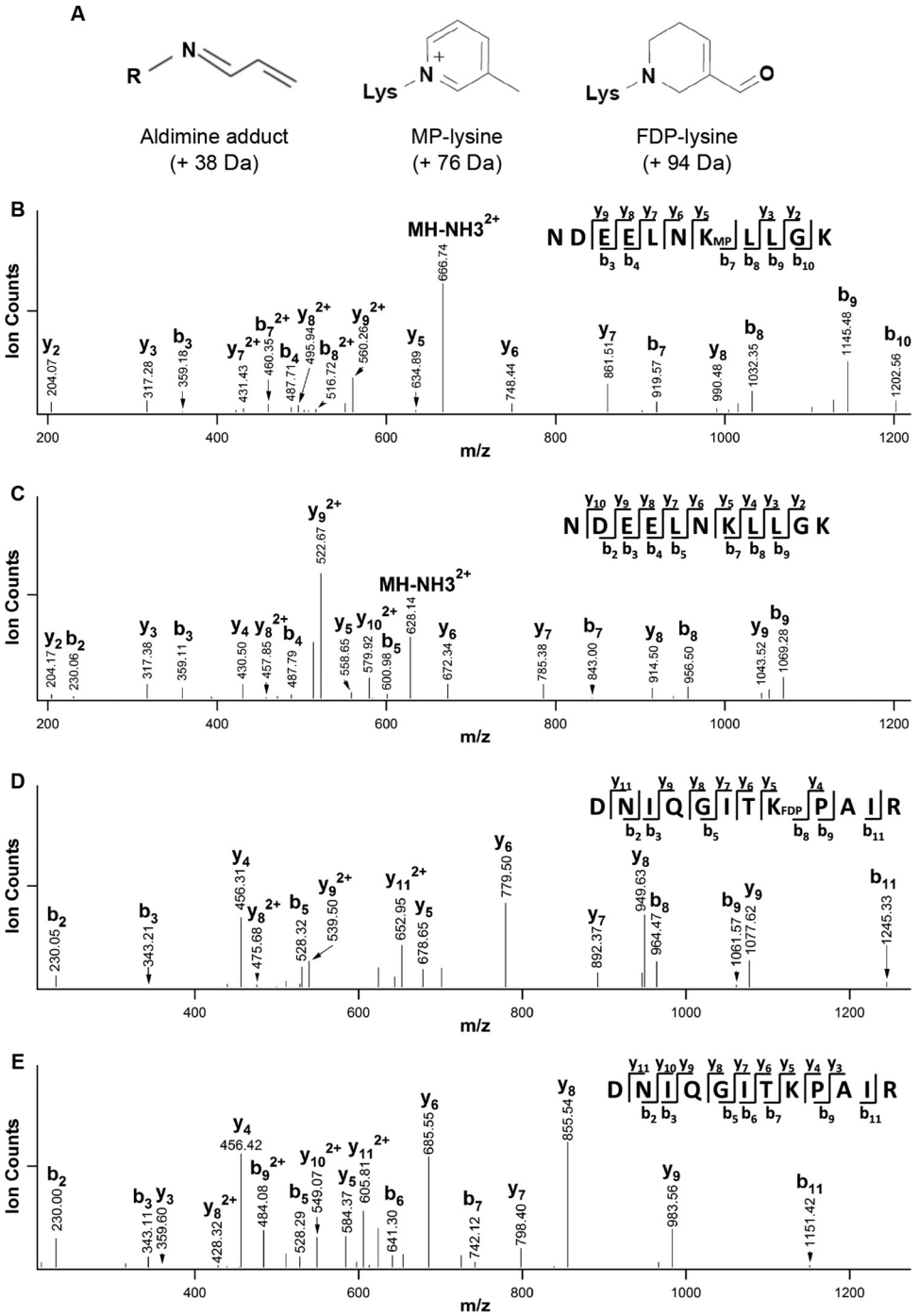

FIG 1 Identification of Acr-modified lysines in recombinant H2A and H4 by LC-MS/MS. (A) Acr forms three major adducts with histone lysine residues: aldimine-modified lysine (A-lysine) with a mass addition of 38 Da, MP-modified lysine (MP-lysine) with a mass addition of 76 Da, and FDP-modified lysine (FDP-lysine) with a mass addition of 94 Da. These three types of mass addition can be detected by LC-MS/MS. (B, C) Identification of Acr-modified lysines in recombinant H2A by LC-MS/MS. Acr-treated H2A was separated by 14% SDS-PAGE and subjected to in-gel digestion with trypsin. The digestion products obtained were analyzed by LC-MS/MS to identify possible Acr-modified peptides. The peptide corresponding to Acr-modified $_{90}$NDEELNK(MP)LLGK$_{100}$ (MH_2^{+2} 674.86) is shown in panel B. The observation of a series of y (y_2, y_3, y_5~y_9) and b (b_3, b_4, b_7~b_{10}) ions identified this peptide with a sequence of $_{90}$NDEELNK(MP)LLGK$_{100}$, in which K96 has a mass addition of 76 Da, corresponding to an MP-modified lysine. (C) The unmodified peptide $_{90}$NDEELNKLLGK$_{100}$ (MH_2^{+2} 636.84) from H2A identified by LC-MS/MS. (D, E) Identification of Acr-modified lysines in recombinant H2A and H4 by LC-MS/MS. (D) The peptide corresponding to Acr-modified $_{25}$DNIQGITK(FDP)PAIR$_{36}$ (MH_2^{+2} 710.40) from H4 identified by LC-MS/MS. The observation of a series of y (y_4~y_9, y_{11}) and b (b_2, b_3, b_5~b_7, b_9, b_{11}) ions identified this peptide sequence as $_{25}$DNIQGITK(FDP)PAIR$_{36}$, in which K32 has a mass addition of 94 Da, corresponding to an FDP-modified lysine. (E) The unmodified peptide $_{2}$DNIQGITKPAIR$_{36}$ (MH_2^{+2} 663.38) from H4 identified by LC-MS/MS.

TABLE 1 Summary of Acr-modified peptides identified in recombinant H2A and H4 by LC-MS/MS[a]

Peptide source and no.	Sequence	ΔM[b] (Da)
H2A		
1	$_{89}$NDEELNK(FDP)LLGR$_{99}$	+94
2	$_{89}$NDEELNK(MP)LLGR$_{99}$	+76
3	$_{36}$K(MP)GNYAER$_{42}$	+76
H4		
1	$_{4}$GK(MP)GGKGLGK$_{12}$	+76
2	$_{4}$GKGGK(MP)GLGK$_{12}$	+76
3	$_{9}$GLGK(MP)GGAK$_{16}$	+76
4	$_{21}$VLRDNIQGITK(MP)PAIR$_{35}$	+76
5	$_{24}$DNIQGITK(FDP)PAIR$_{35}$	+94
6	$_{56}$GVLK(MP)VFLENVIR$_{77}$	+76
7	$_{56}$GVLK(FDP)VFLENVIR$_{77}$	+94
8	$_{68}$DAVTYTEHAK(MP)R$_{78}$	+76
9	$_{68}$DAVTYTEHAK(A)R(A)$_{78}$	+38, +38
10	$_{79}$K(MP)TVTAMDVVYALK$_{91}$	+76
11	$_{78}$RK(FDP)TVTAM(oxidation)DVVYALK$_{91}$	+94
12	$_{80}$TVTAMDVVYALK(MP)R$_{92}$	+76
13	$_{80}$TVTAMDVVYALK(FDP)R$_{92}$	+94

[a] H2A and H4 treated with 50 μM Acr were separated by PAGE, the corresponding gel bands were excised and digested with trypsin, and the resultant peptides were extracted and subjected to LC-MS/MS analysis. The MP- and FDP-modified peptides were identified in both H2A and H4 samples, and an aldimine (A)-modified peptide was also identified in H4 samples. Peptides 1 and 3 show the identification of H4K5MP and K12MP, respectively, demonstrating that both H4K5 and H4K12, two lysine residues critical for histone nuclear import, could be modified by Acr.
[b] ΔM, mass difference.

TABLE 2 Summary of Acr-modified H4 peptides isolated from BEAS-2B cells exposed to Acr by LC-MS/MS[a]

Peptide no.	Sequence	ΔM[b] (Da)	Protein name
1	$_{4}$GK(A)GGK(MP)GLGKGGAK(D)$_{16}$	+38, +76	H4
2	$_{0}$MSGRGK(A)GGK(MP)GLGK$_{12}$	+38, +76	H4
3	$_{9}$GLGK(FDP)GGAK(A)R$_{17}$	+94, +38	H4

[a] The ~55-kDa gel band in the FDP-K IP lane in Fig. 2A was excised and digested with trypsin, and the resultant peptides were extracted and subjected to LC-MS/MS analysis. The aldimine (A)-, MP-, and FDP-modified peptides were identified. Peptides 1 to 3 show the identification of lysine modifications by Acr at the N terminus of H4, demonstrating that both H4K5 and H4K12, two lysine residues critical for histone nuclear import, are modified by Acr *in vivo*. D, dimethyl.
[b] ΔM, mass difference.

after *in vitro* reaction with recombinant histones (Fig. 1). However, this cannot mimic *in vivo* conditions well. To identify Acr-modified histone sites in cells treated with Acr, total histones were isolated by acid extraction from BEAS-2B cells following Acr exposure and subjected to mass spectrometry. BEAS-2B cells were treated with 100 μM Acr for 2 h because our previous cytotoxicity analysis showed >90% cell viability under those conditions and that >80% cell viability was considered to give meaningful outcomes in *in vitro* toxicogenomic studies (23). Moreover, the concentrations of Acr in respiratory tract lining fluid exposed to gas phase cigarette smoke can be as high as 80 μM (57). Shorter treatment times can also minimize the length of time that cells are under stress. No Acr modifications were detected by this method (data not shown). This result was in agreement with our hypothesis that Acr mainly targets cytosolic histones. Since cytosolic histones represent only a small percentage of the total histones, it has been difficult for us to isolate enough histones for detection of the modification. To enrich Acr-modified histones, we pulled down acid extracts with antibodies against FDP-lysine (FDP-K). Interestingly, Western blot analysis showed only one major band with a molecular mass of around 55 kDa detectable by FDP-K antibodies (Fig. 2A). This complex contained histones H3 and H4 since the band overlapped that corresponding to H3 and H4, respectively (Fig. 2A). Besides H3 and H4, histones H2A and H2B were also included in the complex, as evidenced by mass spectrometry detection (data not shown). These results suggest that the complex is probably formed by Acr-mediated cross-links between histone proteins and/or histones and other proteins. We identified three Acr-modified H4 peptides, i.e., $_{4}$GK(A)GGK(MP)GLGKGGAK(D)$_{16}$ (m/z 419.60^{3+}), $_{0}$MSGRGK(A)GGK(MP)GLGK$_{12}$ (m/z 449.58^{2+}), and $_{9}$GLGK(FDP)GGAK(A)R$_{17}$ (m/z 488.29^{2+}) in Acr-treated cells (Table 2). While lysines 5 and 16 were aldimine modified, lysines 8 and 12 were MP and FDP modified, respectively. The results indicate that lysines only in the N-terminal tail seemed to be modified by Acr in cells. A representative MS/MS spectrum of an Acr-modified peptide, $_{4}$GK(A)GGK(MP)GLGKGGAK(D)$_{16}$ (MH_3^{+3} 419.60), from H4 is shown in Fig. 2B, in which K5 has a mass addition of 38 Da and K8 has a mass addition of 76 Da, corresponding to aldimine- and MP-modified lysines, respectively. These data confirm the formation of Acr-lysine histone adducts in cells.

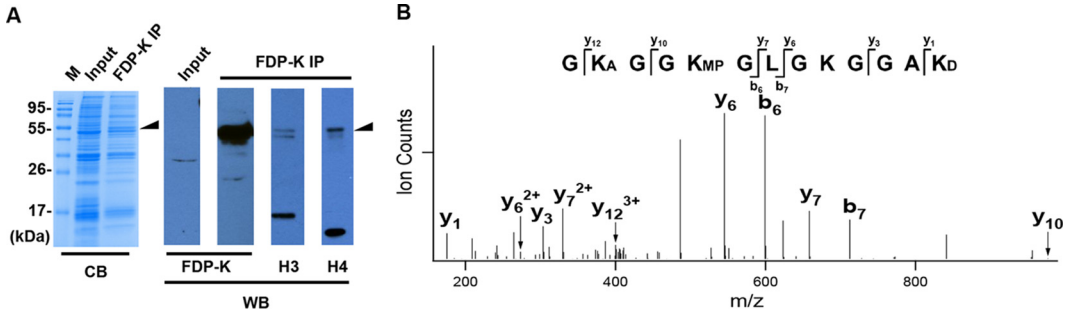

FIG 2 Identification of Acr-modified histone lysines in cells exposed to Acr. (A) FDP-K IP was carried out to enrich Acr-modified histones from acid extracts of BEAS-2B cells. Coomassie blue (CB) staining and Western blot (WB) analysis of FDP-K IP sample demonstrate an ~55-kDa band containing FDP-K, H3, and H4. The ~55-kDa gel band was excised and digested with trypsin, and the resultant peptides were extracted and subjected to LC-MS/MS analysis to determine their composition and possible Acr-modified histone lysines. Lane M, molecular size markers. (B) The peptide corresponding to Acr-modified $_{4}$GK(A)GGK(MP)GLGKGGAK(D)$_{16}$ ($MH3^{+3}$ 419.60) from H4 identified by LC-MS/MS. A, aldimine; D, dimethyl.

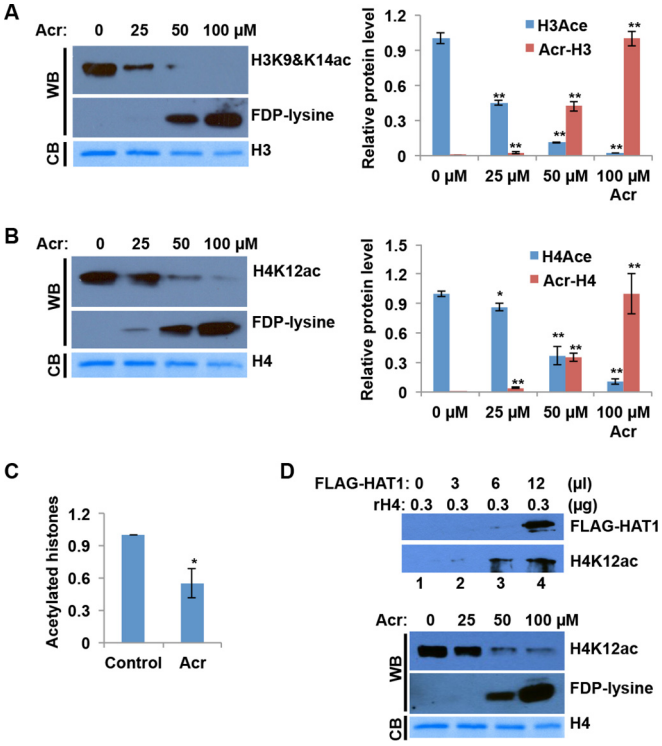

FIG 3 Acr-modified histones are resistant to acetylation. (A and B) Recombinant histone H3 (A) or H4 (B) was treated with Acr overnight prior to HAT reaction with CBP. The samples obtained were subjected to Western blot (WB) analysis with antibodies specific for H3K9&K14ac, H4K12ac, and FDP-lysine, which represent Acr-lysine adducts. Band intensities were quantified with ImageJ software. For comparison, the levels of H3ac/H4ac in lane 1 and Acr-H3/Acr-H4 in lane 4 were set as 1. The data shown are the mean values ± SD from three independent experiments. *, $P < 0.05$; **, $P < 0.01$. CB, Coomassie blue. (C) Histone peptides were treated with Acr (0 and 100 μM) at 37°C overnight. After Acr was removed from the reaction mixture, Acr-treated and untreated histones were subjected to HAT assays with the EpiQuick HAT activity/inhibition assay kit. Cytosolic fractions from normal BEAS-2B cells were used as enzymatic sources. The data shown are the mean values ± SD from assays performed in triplicate. *, $P < 0.05$. (D, top) Recombinant histone H4 was treated with Acr overnight prior to HAT reaction with different dose of FLAG-HAT1. The samples obtained were subjected to Western blot analysis with antibodies specific for H4K12ac and FDP-lysine, which represent Acr-lysine adducts. (D, bottom) Experiments were carried out as described for panel B, except that FLAG-HAT1 replaced GST-CBP as an enzyme source.

Acr-modified histone lysines are resistant to acetylation by HAT. We have shown that Acr forms adducts with histone lysines. To investigate how Acr-histone lysine adducts affect physiological lysine modifications, we performed *in vitro* HAT activity assays with recombinant CBP HAT. We first treated recombinant H3 and H4 with Acr. Western blot analysis shows the formation of FDP-K adducts following Acr treatment (Fig. 3A and B). After complete dialysis, H3 and H4 treated or not treated with Acr were subjected to HAT assays. In the absence of Acr, CBP was able to acetylate H3K9&14 and H4K12 efficiently, whereas this acetylation was inhibited remarkably by Acr exposure (Fig. 3A and B). Moreover, the levels of acetylation were negatively correlated with the amount of Acr-lysine adducts, indicating that inhibition of H3 and H4 acetylation directly associates with the formation of Acr-lysine adducts.

To test whether Acr-modified histones are resistant to acetylation by another HAT(s) in addition to CBP, we applied cytosolic fractions from BEAS-2B containing HAT1 specific for H4K5,12 acetylations in HAT activity/inhibition assays. Less acetylated histone substrate was detected when an Acr-pretreated substrate was used in the assays than with the untreated control (Fig. 3C). To further examine how type B HAT affects the acetylation of Acr-modified histones, we transfected a FLAG-tagged HAT1 plasmid into BEAS-2B cells and purified FLAG-HAT1 by FLAG affinity gel purification. The upper part of Fig. 3D shows that purified FLAG-HAT1 was able to acetylate recombinant histone H4 *in vitro*. We then treated recombinant histone H4 with different concentrations of Acr and subjected it to *in vitro* HAT assays with purified FLAG-HAT1. The lower part of Fig. 3D shows that Acr modification reduced the level of H4K12ac induction by FLAG-HAT1. These results support the idea that Acr-modified histone lysines are refractory to acetylation by HAT.

Acr exposure does not change CBP HAT activity *in vitro* and "total" HAT activity *in vivo*. Previously, we demonstrated that Acr exposure downregulates N-terminal tail acetylations of cytosolic histones H3 and H4 in cells (23). This is likely due to the formation of Acr-histone adducts, which prevents the sites from being normally acetylated. In addition to Acr-histone adduct formation, the reduced expression of modifying enzymes or altered enzyme activity might also contribute to the reduction of histone modifications following Acr exposure. To test this, we first measured the expression levels of HAT1, a HAT specific for free H4K5&K12, before and after Acr treatment. Figure 4A shows that HAT1 expression in BEAS-2B cells did not decrease following Acr exposure. We next tested if HAT activity is affected by Acr exposure *in vitro* and in cells. Recombinant GST-CBP was treated with different concentrations of Acr and subjected to HAT assays with recombinant histone H4 as the substrate. In the absence of Acr, GST-CBP was able to acetylate histone H4, as evidenced by increased levels of H4K12ac and H4K5ac (Fig. 4B, compare lanes 1 and 2). Intriguingly, the levels of H4 acetylation remained unchanged in the presence of Acr (Fig. 4B, lanes 2 to 5), indicating that CBP HAT activity was not changed by Acr modification of the enzyme. Since HAT1 specifically acetylates free H4K5&12, we next examined the effect of Acr on the activity of HAT1. We treated purified FLAG-HAT1 with different concentrations of Acr (0, 25, 50, and 100 μM) for 2 h and subjected it to a HAT activity assay. As shown in Fig. 4C, the activity was slightly reduced only when 100 μM Acr was used.

We next examined the effects of Acr on HAT activity in cells. We isolated cytosolic fractions from cells treated or not treated with Acr and measured the HAT activities of these fractions with an EpiQuick HAT activity/inhibition assay kit. When cytosolic fractions isolated in the presence of sodium butyrate, an inhibitor of histone deacetylases (HDACs), were used, a smaller amount of acetylated histone substrate was detected following Acr exposure than in the untreated control (Fig. 4D), indicating that HAT activity in cells might be affected by Acr exposure. This is partially in agreement with *in vitro* results (lane 5 in Fig. 4C). However, HAT activity remained the same before and after Acr treatment when the cytosolic fractions were isolated in the absence of sodium butyrate (Fig. 4D), indicating that the cytosolic "total" HAT activity, i.e., the net changes in the dynamic addition and removal of acetyl groups by HATs and HDACs, remains the same in Acr-treated and untreated cells. Together, the data support the idea that reduced histone posttranscriptional modifications (PTMs) by Acr

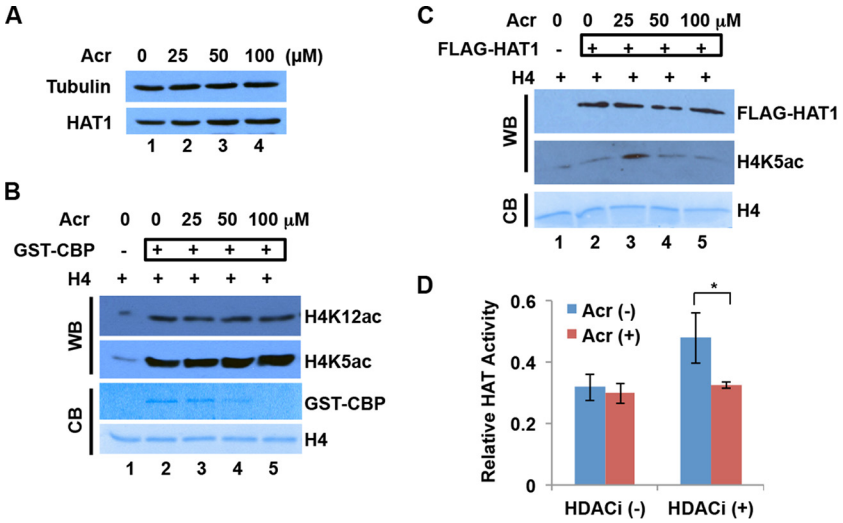

FIG 4 Effects of Acr exposure on HAT expression and activity. (A) HAT1 protein levels were not changed by Acr exposure in BEAS-2B. BEAS-2B cells were treated with Acr for 2 h. Cytosolic fractions were then extracted for Western blot analysis with HAT1 antibody. Tubulin was used as the loading control. (B) The HAT activity of GST-CBP was not affected by Acr exposure. Recombinant GST-CBP was treated with Acr overnight and then used for a HAT activity assay with recombinant H4 as the substrate. The acetylation reaction was monitored by Western blotting (WB) with H4K5ac and H4K12ac antibodies. Coomassie blue (CB) staining of GST-CBP and H4 is shown. (C) The HAT activity of FLAG-HAT1 was not affected by Acr exposure *in vitro*. Purified FLAG-HAT1 was treated with Acr overnight and then used for a HAT activity assay with recombinant H4 as the substrate. The FLAG-HAT1 level was determined by Western blotting with FLAG antibody. The acetylation reaction was monitored by Western blotting with H4K5ac antibody. Coomassie blue staining of H4 is shown. (D) The "total" HAT activity of cytosolic fractions was not changed by Acr exposure. After BEAS-2B cells were treated with 100 μM Acr for 2 h or not treated with Acr, cytosolic fractions were isolated in the absence (−) or presence (+) of sodium butyrate, an HDAC inhibitor (HDACi). HAT assays were performed with histone peptides as substrates and cytosolic fractions as an enzyme source. The average values ± SD of three independent experiments are presented. *, $P < 0.05$.

exposure in cells are most likely due to the formation of Acr-histone adducts.

Acr modification of histone chaperone ASF1B has subtle effects on its interaction with H3-H4. Chromatin assembly is mainly regulated by histone modifications and histone chaperone proteins. We have demonstrated that Acr inhibits histone acetylations likely through the formation of Acr-histone lysine adducts at the sites important for chromatin assembly. However, it is not known whether Acr also targets histone chaperones, thereby compromising chromatin assembly, possibly by interfering with interactions between histone chaperones and histones. To determine how the Acr modifications of histone chaperones affect their interaction with histones, we performed *in vitro* GST pulldown assays with GST-fused ASF1B and histone H3-H4 tetramers. We first treated GST-ASF1B with different concentrations of Acr. The formation of Acr-ASF1B adducts was confirmed by Western blotting with an FDP-K antibody (Fig. 5A). Acr-modified GST-ASF1B was then incubated with H3-H4 tetramers, and the GST-ASF1B complex was pulled down by GST beads, followed by Western blotting to determine the interaction between ASF1B and H3-H4 by measuring the levels of histone H3 in the complex. In the absence of Acr, GST-ASF1B interacted with H3-H4, whereas GST alone failed to bind to H3-H4 (Fig. 5A, compare lanes 6 and 7). Importantly, the level of H3 in the Acr-modified GST-ASF1B complex was comparable to that in the untreated ASF1B complex and remained unchanged as the Acr dose increased (Fig. 5A), suggesting that Acr modification of ASF1B has subtle effects on the interaction between ASF1B and histones. To analyze whether Acr-histone adducts have similar effects on the interaction between ASF1B and histones, we first treated H3-H4 tetramers with Acr and then tested their binding to untreated GST-ASF1B by GST pulldown assays. The binding of Acr-modified H3-H4 to ASF1B was not changed at the 25 and 50 μM doses of Acr. The interaction was slightly decreased when the tetramers were treated with 100 μM Acr (Fig. 5B). However, this could be interpreted in light of the fact that there is less input H3 in this particular sample, probably because of heavy Acr modifications. Taking these results together, we conclude that Acr modification itself has little or no effect on protein-protein interactions.

Acr exposure disrupts the association of histones with histone chaperone and translocator proteins in cells. The interaction between histones and the histone chaperone ASF1B was slightly decreased only when histone proteins were treated with 100 μM Acr *in vitro*. Exposure of cells to 100 μM Acr should not generate the same amount of Acr-ASF1B or Acr-histone adducts as seen after the *in vitro* treatment of ASF1B or histones with 100 μM Acr, since in cells Acr will first be scavenged by glutathione and the rest will react with other cytosolic proteins. Therefore, Acr-ASF1B adducts or Acr-histone adducts themselves may have no effects on the associations in cells exposed to 100 μM Acr. However, reduction of H4K5,12 acetylations due to the formation of Acr adducts might have an impact on the interaction because it has been shown that these modifications are required for the association of histones with ASF1B and importin 4 (31, 33, 46). To test this possibility, we first established BEAS-2B cells stably expressing FLAG-tagged H3 and determined the levels of H3-interacting proteins before and after Acr exposure by FLAG IP, followed by Western blotting assays. In agreement with our previous results, H4K12ac was downregulated by Acr exposure (compare lanes 1 and 4 in Fig. 5C). Moreover, the levels of importin 4, ASF1B, and HAT1 expression (compare lanes 1 and 4 in Fig. 5C) were not altered upon Acr exposure, indicating that changes in

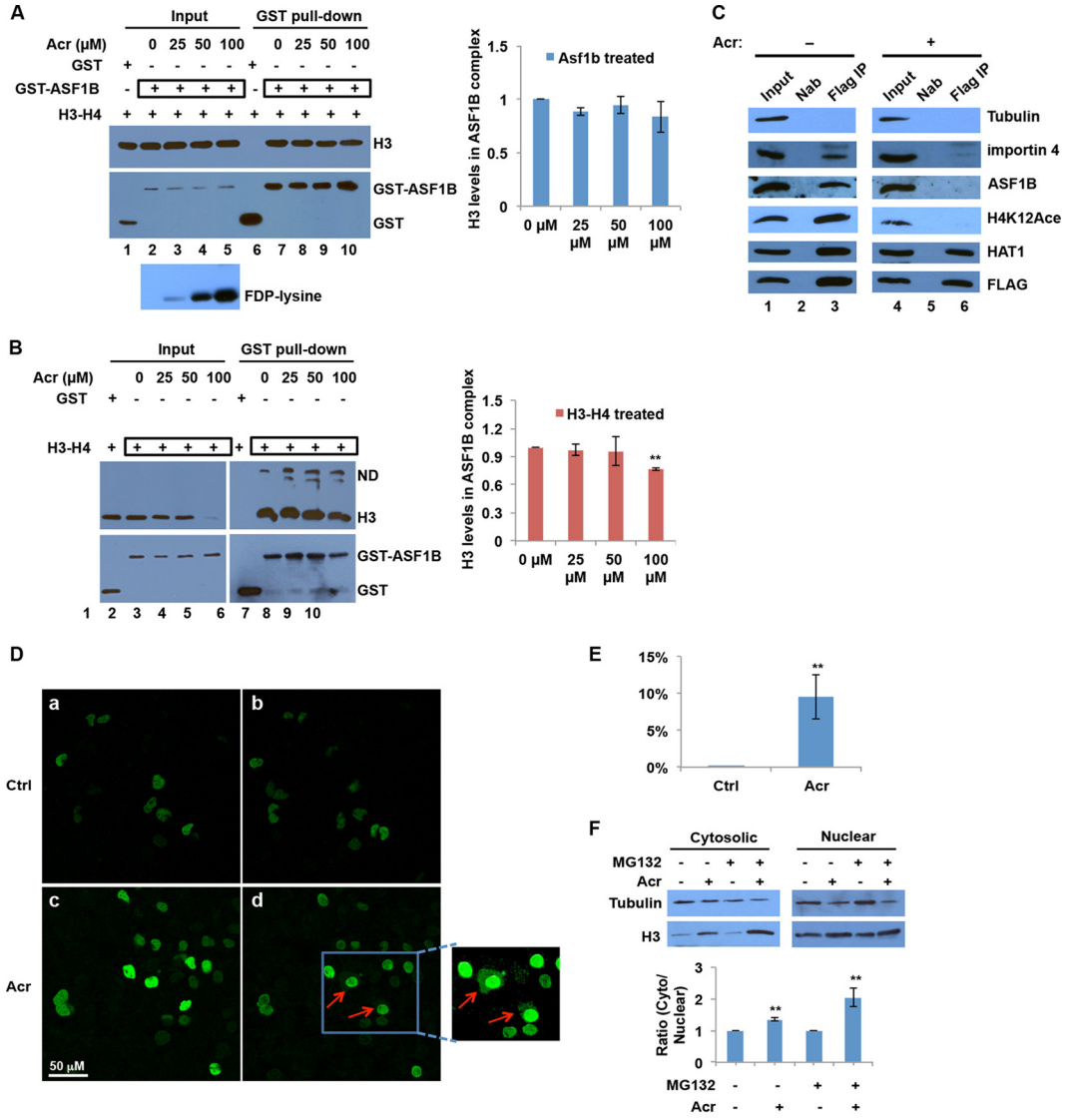

FIG 5 Acr inhibits nuclear import of histones by disrupting the interaction between histones and their translocator protein. (A, B) Effects of Acr modification on the interaction between ASF1B and histones *in vitro*. GST-ASF1B was treated with Acr, mixed with H3-H4 tetramers, and then subjected to GST pulldown assays, followed by Western blotting with the antibodies indicated (A). H3-H4 tetramers were treated with Acr and then mixed with GST-ASF1B and subjected to GST pulldown assays (B). Bar graphs showing relative quantification of histone H3 levels in GST pulldown samples normalized to ASF1B. The data shown are the mean values ± SD from three independent experiments. **, $P < 0.01$. (C) Disruption of association of histones with a histone chaperone and a translocator protein in cells exposed to Acr. BEAS-2B cells that stably express FLAG-tagged histone H3 were treated with 100 μM Acr for 2 h or not treated with Acr. Cytosolic fractions were isolated and subjected to FLAG IP, followed by Western blotting with the antibodies indicated. Nab, no antibody (negative control). (D, E) Acr exposure inhibits the nuclear import of nascent histones. (D) Time-lapse experiments were performed to study the effects of Acr on nascent histone nuclear import. EGFP-H3 expression was induced overnight in inducible UTA6-EGFP-H3 cells. The cells were treated with 20 μM MG132 for 2 h and then treated with 100 μM Acr for an additional 2 h (Acr) or not treated with Acr (Ctrl). The cellular distribution of EGFP-H3 was monitored with an immunofluorescence confocal microscope. (a, b) Untreated UTA6-EGFP-H3 cells at 0 (a) and 120 (b) min. (c, d) Acr-treated UTA6-EGFP-H3 cells at 0 (c) and 120 (d) min. Newly synthesized EGFP-H3 was retained in the cytoplasm following Acr exposure, as indicated by the red arrow. (E) Percentages of cells with retained GFP signals in the cytoplasm. The number of cells with EGFP-H3 retained in the cytoplasm was determined and divided by the total cell number. The data shown are the mean values ± SD from four independent experiments. **, $P < 0.01$. (F) Ratio of cytosolic to nuclear H3 distribution following Acr exposure. Cells were treated or not treated with MG132 before and after Acr exposure. The cytosolic and nuclear fractions were extracted and subjected to Western blot analysis with H3 antibodies. Band intensities were quantified with ImageJ software. Each column shows the ratio of the H3 level in the cytoplasm to that in the nucleus. The data shown are the mean values ± SD from four independent experiments. **, $P < 0.01$.

protein levels were not attributable to the changes in interactions between histones and these proteins. As expected, the interaction between H3 and ASF1B decreased dramatically following Acr exposure (compare lanes 3 and 6 in Fig. 5C). The association of H3 with importin 4 was also disrupted by Acr treatment (Fig. 5C). However, the levels of HAT1 in H3 complex were not altered upon Acr exposure, again supporting the idea that reduction of H4K12ac levels is probably due not to aberrant HAT expression or activity but to Acr-histone lysine adduct formation. Disruption of associations of histones with histone translocators and chaperone

proteins may reflect a mechanism by which Acr regulates chromatin assembly.

Inhibition of histone nuclear import by Acr. Histone H3 failed to properly interact with importin 4 in Acr-exposed cells (Fig. 5C), suggesting that histone translocation from the cytoplasm to the nucleus might be affected by Acr treatment. To visualize the dynamic movement of newly synthesized histones from the cytoplasm to the nucleus, we combined the inducible GFP-tagged histone expression system with time-lapse microscopy. We first generated a stable UTA6 human osteosarcoma cell line with tetracycline-repressive GFP-tagged H3 (GFP-H3). After inducing GFP-H3 expression by removing tetracycline from the medium, we monitored histone nuclear import by comparing the cellular localization of GFP-H3 signals before and after Acr treatment. Aggregation of Acr-modified histones may undergo degradation. Therefore, to maximize the intensity of the GFP signals that we can detect, we used the proteasome inhibitor MG132 to prevent possible GFP-H3 degradation. We treated the cells with 100 μM Acr and monitored the cellular distribution of GFP-H3 for 2 h by time-lapse microscopy. Histones fused to GFP have been used as a marker for the nucleus in the staining of living cells. Not surprisingly, GFP-H3 signals were exclusively localized in nuclei and the intensities remained unchanged in untreated cells, indicating that newly synthesized histones were normally translocated into the nucleus in the absence of Acr (Fig. 5D, a and b). In contrast, in the presence of Acr, clear GFP signals accumulated in the cytoplasm of several cells and GFP signals in nuclei were generally lower than in the control (Fig. 5D, c and d). We calculated the number of cells showing retained signals in the cytoplasm at the 0- and 2-h time points. About 10% of the cells displayed GFP signals in the cytoplasm following this treatment (Fig. 5E). We next quantified the ratio of cytosolic to nuclear distribution of H3 by Western blotting. Figure 5F shows that the ratio was increased by Acr exposure, especially in the presence of MG132, indicating that there is an accumulation of histone proteins in the cytoplasm following Acr exposure and that the aggregates trigger proteosomal degradation. These results suggest that histone translocations were notably inhibited in cells following Acr exposure.

Acr exposure inhibits RSF-mediated chromatin assembly that requires histone acetylation for efficient assembly. To investigate the effects of Acr-protein adducts on chromatin assembly, we carried out *in vitro* plasmid supercoiling assays. ASF1B was incubated with core histones and then mixed with relaxed circular DNA. Untreated ASF1B was shown to introduce supercoils into circular DNA (lane 7 in Fig. 6A). Remarkably, Acr-modified ASF1B was able to introduce supercoils as efficiently as untreated ASF1B did (lanes 7 to 9 in Fig. 6A). Furthermore, ASF1B also efficiently induced supercoils into relaxed plasmid DNA in the presence of core histones treated with 25 or 50 μM Acr prior to the reaction (lanes 1 to 3 in Fig. 6A), indicating that the chromatin assembly activity of ASF1B was not affected by either Acr-modified histones or Acr-modified ASF1B. Together, our results suggest that Acr modifications of either histones or chaperone proteins have no direct effect on plasmid supercoiling that does not require histone acetylations.

To further explore the molecular mechanisms that underlie Acr-induced inhibition of chromatin assembly, we performed unique RSF chromatin assembly assays (Fig. 6B) (56, 58). RSF is a histone chaperone complex containing Rsf-1 and SNF2h subunits (56, 59). Loyola et al. have demonstrated that histone acetylation does not affect the binding of RSF to histones, whereas acetylation of H4, H2A, and H2B is important for the RSF-mediated formation of regularly spaced nucleosomes, although the underlying mechanisms have not been determined (56, 58). These characteristics of the RSF assay make it a perfect system with which to determine whether Acr modification can mimic the acetylation status of histones and to investigate whether downregulation of histone acetylation by the formation of Acr-histone lysine adducts contributes to Acr-mediated aberrant chromatin assembly. To perform RSF assays, a recombinant RSF complex was purified from SF9 cells infected with baculoviruses expressing FLAG-tagged Rsf-1 and hSNF2H (not shown). To prepare acetylated histones, including acetylated H2A/H2B, reconstituted histone octamers were subjected to a HAT reaction with or without the CBP HAT. Purified acetylated or unacetylated histones were then used in RSF chromatin assembly assays (Fig. 6C, middle, lanes 2 and 3). As expected, more regularly spaced MNase DNA ladders were detected when acetylated histones were used than with the control (Fig. 6C, top, compare lanes 2 and 3). Next, we treated histones with Acr prior to HAT assays. As shown in the middle of Fig. 6C, the histone acetylation level was remarkably decreased by pretreatment of histones with Acr (compare lanes 3 and 4). Consequently, less nucleosomal DNA ladders were observed when Acr-treated histones were used than with the untreated control (Fig. 6C, top, lanes 3 and 4) and the pattern resembled an unacetylated histone sample (Fig. 6C, top, compare lanes 2 and 4). Moreover, as shown in Fig. 6D, dose-dependent inhibition of RSF-mediated chromatin assembly by Acr was also observed. These data suggest that hypoacetylation of histones due to the formation of Acr-histone adducts is the major contributor to Acr-induced inhibition of chromatin assembly.

DISCUSSION

Previously, we reported that Acr, a major component of cigarette smoke and cooking fumes, forms adducts with lysines on histone proteins and compromises chromatin assembly pathways, probably by downregulating N-terminal tail acetylations of newly synthesized histones (23). In the present study, we have addressed possible mechanisms underlying Acr-induced inhibition of chromatin assembly. We found that the formation of Acr-histone adducts itself had little or no effect on protein-protein interactions and chromatin assembly *in vitro*. The reduction of physiological modifications due to the formation of Acr-histone lysine adducts at sites important for histone nuclear import and chromatin assembly seemed to be the major cause of Acr-mediated inhibition of chromatin assembly pathways.

We previously demonstrated that the levels of H3K9&14 acetylations and H4K12 acetylation are reduced in cells exposed to Acr and hypothesized that the reduction is, at least in part, a result of the formation of Acr-histone adducts at those sites (23). In this study, we used mass spectrometry to determine the sites of Acr-lysine adducts on histones. We found that Acr reacts with the majority, but not all, of the lysines on H4 *in vitro*, including lysines 5, 12, 79, and 91, which are sites believed to be important for chromatin assembly (Table 1) (32, 33, 38). Interestingly, Acr formed adducts with lysines only in the N-terminal tail of H4, including 5 and 12, in cells (Table 2). We further utilized HAT assays to test how Acr modifications influence lysine acetylation by HAT. Our data revealed that Acr modifications of recombinant histones prevent lysine acetylation by the CBP HAT in a dose-

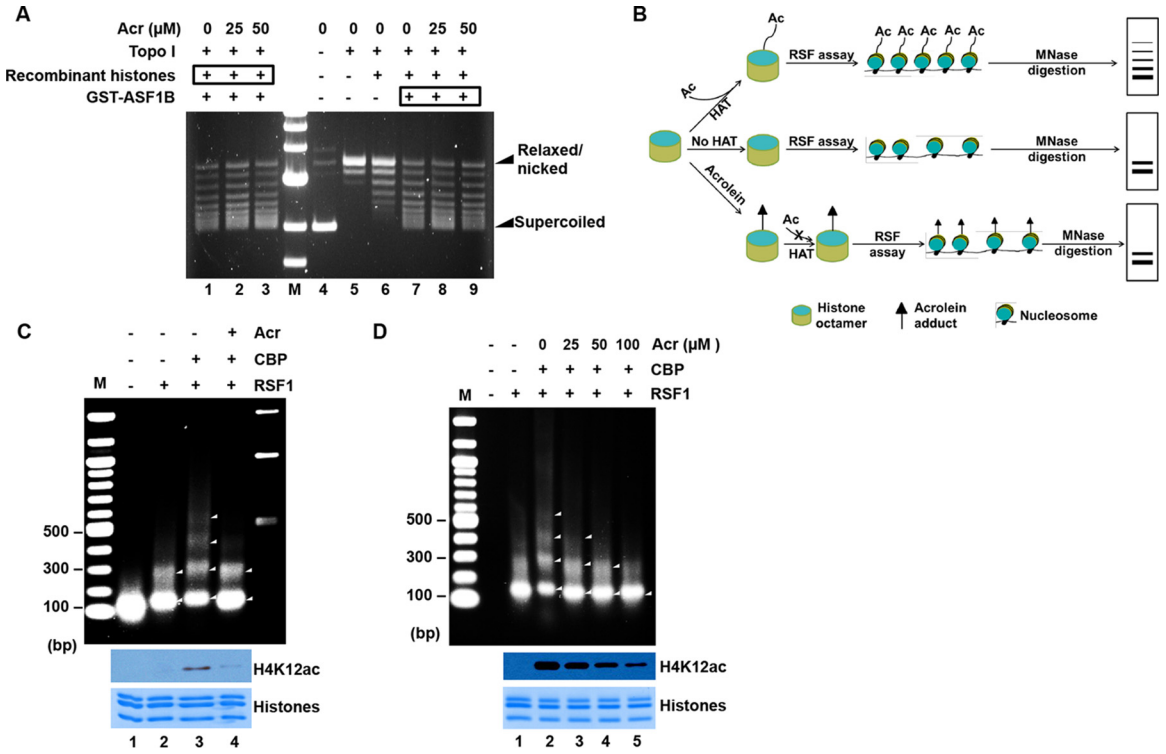

FIG 6 Exposure of histones to Acr inhibits RSF-mediated chromatin assembly. (A) ASF1B-mediated plasmid supercoiling is not changed by Acr exposure. Plasmid supercoiling was not affected by the exposure of either histones or ASF1B to Acr. For lanes 1 to 3, reconstituted histone octamers were treated with Acr prior to reaction and then subjected to *in vitro* plasmid supercoiling assays. For lanes 7 to 9, GST-ASF1B was treated with Acr and then mixed with reconstituted histone octamers for plasmid supercoiling assays as described in Materials and Methods. A result representative of three independent experiments is shown. (B) Schematic representation of RSF chromatin assembly assays. (Top) Acetylation (Ac) of histones, especially H2A-H2B, is critical for the efficient formation of regularly spaced nucleosomes mediated by RSF, which generates nucleosomal DNA arrays when analyzed by partial MNase digestion. (Middle) With unacetylated histones, chromatin assembly is greatly inhibited, forming fewer regularly spaced nucleosomes, which are more accessible by MNase digestion, and generates only up-to-2-mer arrays. (Bottom) Since Acr-modified histones are resistant to acetylation by HAT (Fig. 3), the Acr-treated histones, similar to unacetylated histones, are assembled into chromatin efficiently by RSF, generating fewer DNA arrays when analyzed by partial MNase digestion. (C) Partial MNase digestion analysis of RSF assays with Acr-treated histones. Core histones (bottom, Coomassie blue staining) were treated with Acr (lane 4) or not treated with Acr (lanes 1 to 3) and subjected to acetylation in the presence (lanes 3 and 4) or absence (lanes 1 and 2) of CBP, generating acetylated or less acetylated histones, as evidenced by Western blotting with antibodies to H4K12ac (middle). These histones were then used in RSF chromatin assembly assays, followed by partial MNase digestion. DNA was extracted and analyzed by agarose gel electrophoresis. While larger-than-4-mers of polynucleosomal DNA ladder were observed when acetylated histones were used (lane 3), only bands indicative of monomers and dimers were detected when Acr-exposed histones were used (lane 4). Lane M, DNA size markers. (D) Dose-dependent effects of Acr on RSF chromatin assembly. The assays were carried out as for panel C, except that different doses of Acr were used.

dependent manner (Fig. 3). The results are in agreement with those seen upon formaldehyde exposure of recombinant histone H4 (60). These data support the idea that the observed reduction of H4K12 acetylation and probably H3K9&14 acetylations in cells exposed to Acr may occur because of the formation of Acr-lysine adducts. However, as a highly reactive aldehyde, Acr might also target a histone-modifying enzyme(s) to alter either its expression or its function, leading to changes in histone modifications following Acr exposure. Western blot analysis showed no changes in the expression of HAT1 (Fig. 4), which is specific for H4K5,12 acetylations (33). The levels of HAT1 mRNA were also not changed by Acr exposure (not shown). In addition, the expression of HAT1 was only slightly reduced following low-dose (5 μM) treatment, and only on day 7, while the H4K12ac level started to decrease from day 5 (23). Notably, exposure of the CBP HAT to Acr prior to the reaction had no effect on CBP HAT activity (Fig. 4), suggesting that even though Acr forms adducts with HATs in cells, it is not likely to interfere with their activities. To test this possibility, we isolated cytosolic fractions from BEAS-2B cells treated or not treated with Acr and used them as enzyme sources in HAT assays. The "total" HAT activity, i.e., the net changes in the dynamic addition and removal of acetyl groups by HATs and HDACs, remained the same before and after Acr exposure (Fig. 4). The data support the idea that reduced histone PTMs caused by Acr exposure are most likely due to the formation of Acr-histone adducts. In our previous study, we showed that treatment of BEAS-2B cells with 5 μM Acr, which is physiologically relevant in terms of the amounts of Acr generated by about one cigarette, was able to reduce cytosolic H4K12ac and increase chromatin accessibility (23). Thus, the mechanisms found in this study are likely applicable to the low concentration as well.

Acetylation of the histone tails may affect chromatin assembly pathways by two mechanisms. First, some acetylations, such as H4K5,12ac, are required for the association of histones with translocator protein importin 4 and histone chaperone ASF1 to affect histone nuclear translocation and histone transfer (45, 46). Second, the modifications may directly affect chromatin assembly processes by facilitating the deposition of histones to DNA and/or

regulating nucleosome spacing (56). Whereas the expression levels of ASF1B and importin 4 were not changed following Acr treatment, Acr exposure dramatically decreased the association of H3/H4 with ASF1B and importin 4 in BEAS-2B cells (Fig. 5C). Accordingly, time-lapse microscopy analysis showed decreased GFP signal levels in the nuclei and retained histones in the cytoplasm of Acr-exposed cells but not in those of untreated cells (Fig. 5D), which suggests inhibition of histone nuclear import. In contrast, the interaction between H3/H4 and HAT1 was not changed by Acr. Since Acr-histone adducts or Acr-ASF1B adducts themselves could affect the associations independently of histone acetylation status, we also performed GST pulldown assays to examine how protein-protein interactions are affected by Acr exposure. We found that Acr modifications of either histones or ASF1B had little or no impact on the association of histones with ASF1B (Fig. 5), suggesting that it is not Acr modifications themselves but reduction of physiological acetylations due to Acr adduct formation that is critical for disruption of histone/histone chaperone interactions. In addition, strong interactions between histone and ASF1B (Fig. 5A) implied that there might be acetylation on recombinant histone proteins. It has been reported that lysine acetylation is abundant in *E. coli* proteins (61). Thus, it is not surprising that bacterial purified recombinant histones get acetylated to some extent. In fact, our Western blot analysis results showed a low level of H4K5ac on recombinant histone H4 even in the absence of CBP (Fig. 4B). However, the acetylation level of recombinant histones seems very low, given that without acetylation by CBP, recombinant histones themselves were not able to form nucleosome arrays in RSF assays (compare lanes 2 and 3 in Fig. 6C). Therefore, it is also possible that histone modifications are required for the interaction between H3/H4 and ASF1B only *in vivo* and not *in vitro*.

We used *in vitro* plasmid supercoiling and RSF chromatin assembly assays to test the effects of Acr on different steps of the chromatin assembly process. RSF chromatin assembly assays require acetylation of H2A and H2B for efficient assembly (56), which enables us to examine whether regulation of histone acetylation status is critical for Acr-mediated inhibition of chromatin assembly. Our data demonstrate that exposure of histones or histone chaperones to Acr has no effect on plasmid supercoiling (Fig. 6A), indicating that Acr modifications themselves cannot change these processes. However, inhibition of histone acetylations, including H2A and H2B, by exposure of histones to Acr prior to HAT reaction greatly compromises the formation of regularly spaced nucleosome arrays mediated by RSF (Fig. 6C and D). These results further support our hypothesis that Acr compromises chromatin assembly pathways via the formation of Acr-lysine histone adducts at the sites important for chromatin assembly, which prevents the sites from being physiologically acetylated.

In theory, Acr could react with nucleophilic amino acid residues such as lysine, arginine, histidine, and cysteine on susceptible proteins, leading to deregulation of protein functions (16, 19, 62). Protein adducts appeared to have less of an impact on protein functions than we previously thought because (i) Acr modifications did not change the enzymatic activity of HATs, even when the protein was treated with a high concentration of Acr, (ii) Acr exposure *in vitro* had little or no effect on protein-protein interactions, and (iii) Acr modifications did not interfere with the histone chaperone activity of ASF1B. In this study, we have found a new mechanism by which Acr modifications affect protein functions; i.e., Acr compromises protein-protein interaction and chromatin assembly by targeting critical sites on proteins and preventing the sites from physiological (functional) modifications.

Another relatively well-studied mechanism is the conformational changes in protein domains caused by targeting of critical residues within the domain by Acr. For instance, IKKβ activity was inactivated by reaction of Acr with an active-site cysteine in the active loop, which induced conformational changes in the loop, rendering adjacent amino acids inaccessible to phosphatases (21). In addition, Wang et al. reported that Acr causes degradation of DNA repair proteins, including XPA, XPC, hOGG1, PMS2, and MLH1, suggesting that protein degradation might be another mechanism whereby Acr-protein adducts change protein functions (15). This is consistent with the results of our time-lapse microscopy analysis showing retained GFP-H3 signals in cytoplasm only when the cells were treated with the proteasome inhibitor MG132 (Fig. 5D and data not shown). The ratio of Acr to cell numbers seemed to be critical for Acr-mediated proteosomal degradation. We propose that, at low concentrations, aldehyde and other electrophiles interfere with protein functions by reacting with critical residues on the proteins, thereby inducing conformational changes in functional domains or preventing the sites from being physiologically modified. At high concentrations, proteins are heavily modified by electrophiles, which trigger protein degradation. It would be important to determine the sites and/or the levels of adducts needed to initiate Acr-mediated proteosomal degradation.

Acr, as an unsaturated aldehyde, could react with nucleophilic sites in proteins such as the sulfhydryl group of cysteine, the imidazole moiety of histidine, and the ε-amino group of lysine (11, 62–64). Acr can also form propano adducts with the guanidine group of arginine (65). Shao et al. used model peptides containing histidine, lysine, and/or arginine to identify the target of Acr (64, 66). They found that Acr targets histidine and lysine but not arginine on the model peptides. Interestingly, although apoA-I contains five histidine residues, they were not able to detect Acr-histidine adducts on apoA-I proteins. In addition, while high levels of FDP-K and low levels of MP-lysine formed in all of the model peptides tested, only MP-lysine was detected when apoA-I was exposed to Acr. These data suggest that the local amino acid environment and protein structure are important for the regulation of Acr reactivity with proteins. In this study, we used recombinant histones H2A and H4 to identify sites of Acr-histone lysine reactions. We found that Acr forms adducts with histones at specific lysine residues. The coverage of lysine residues on H2A and H4 in trypsin-digested samples was 57% (8 out of 14) and 100% (11), respectively. However, of all of the lysine residues identified by mass spectrometry, only a portion of them, 25% (2 out of 8) and 73% (8 out of 11), respectively, were modified by Acr (Table 1), which suggests selectivity of Acr addition by an unknown mechanism.

In vitro studies have shown that self-association of H4 is much stronger than self-association of H2A (67), indicating that tertiary structure may have an impact on the control of Acr-histone lysine adduct formation, given the similar secondary structures of histone proteins. This may also reflect *in vivo* status, since our previous study demonstrated that Acr forms more adducts with histones H3 and H4 than with histones H2A and H2B, as evidenced by protein carbonyl assays (23). A number of studies have dem-

onstrated that adjacent amino acids may direct the modification of specific lysine residues in apoA-I proteins. For example, it was reported that K-226 is the major target of Acr in apoA-I and it was hypothesized that an adjacent negatively charged glutamic acid (Glu-234) could promote electrophilic attack on the side chain of lysines by facilitating deprotonation of the ε-amino group, thereby lowering its pKα and increasing its nucleophilicity (64). Using a peptide that mimics α-helices of apoA-I and apoE, Zheng et al. further reported that an EXXK motif dictates preferential lysine modifications by Acr (68). In future studies, it will be important to investigate whether similar mechanisms are involved in histone modifications by Acr. In addition to the inherent selectivity of Acr, there are also other factors causing the failure of fully reporting all of the Acr-modified sites, including the choice of digestion enzymes, the abundance of modifications, and MS instrument sensitivity.

In summary, we have identified lysine residues on histone H4 that react with Acr *in vitro* and in cells. We also found that Acr modifications themselves are not important for the association of histone proteins with histone chaperones and for chromatin assembly. Abnormal histone acetylations due to the formation of Acr-lysine adducts appear to be attributable to disruption of protein-protein interactions and aberrant chromatin assembly. We propose that prevention of physiological modifications might be a new mechanism whereby Acr-protein adducts perturb cellular processes. In fact, Acr treatment led to S-phase accumulation, as seen in cells with ASF1B knockdown. In combination with its effects on DNA damage and mutagenicity, Acr has a high potential to induce carcinogenesis and other human diseases. Future studies should focus on the global effects of Acr on chromatin structure and gene expression by using high-throughput methodologies such as chromatin immunoprecipitation-DNA sequencing and transcriptome sequencing. Deciphering Acr-induced protein interaction networks and PTM changes by mass spectrometry will provide potential biomarkers and therapeutic target for Acr-related cancers and diseases.

ACKNOWLEDGMENTS

We thank Danny Reinberg, Kazunari K. Yokoyama, Zhiguo Zhang, and Kyosuke Nagata for kindly sharing plasmids.

This work was supported in part by National Institutes of Health grants 1R01ES026138-01 to C.J. and R01GM074830 to L.H. and NIEHS Center of Excellence Pilot Project Program and Career Development grant 5P30ES000260 to H.L. and C.J.

FUNDING INFORMATION

This work, including the efforts of Lan Huang, was funded by HHS | NIH | National Institute of General Medical Sciences (NIGMS) (R01GM074830). This work, including the efforts of Chunyuan Jin, was funded by HHS | NIH | National Institute of Environmental Health Sciences (NIEHS) (1R01ES026138-01). This work, including the efforts of Hongjie Li and Chunyuan Jin, was funded by HHS | NIH | National Institute of Environmental Health Sciences (NIEHS) (5P30ES000260).

REFERENCES

1. **Faroon O, Roney N, Taylor J, Ashizawa A, Lumpkin MH, Plewak DJ.** 2008. Acrolein environmental levels and potential for human exposure. Toxicol Ind Health **24:**543–564. http://dx.doi.org/10.1177/0748233708098124.
2. **Ghilarducci DP, Tjeerdema RS.** 1995. Fate and effects of acrolein. Rev Environ Contam Toxicol **144:**95–146.
3. **Jaganjac M, Prah IO, Cipak A, Cindric M, Mrakovcic L, Tatzber F, Ilincic P, Rukavina V, Spehar B, Vukovic JP, Telen S, Uchida K, Lulic Z, Zarkovic N.** 2012. Effects of bioreactive acrolein from automotive exhaust gases on human cells in vitro. Environ Toxicol **27:**644–652. http://dx.doi.org/10.1002/tox.20683.
4. **Cohen SM, Garland EM, St John M, Okamura T, Smith RA.** 1992. Acrolein initiates rat urinary bladder carcinogenesis. Cancer Res **52:**3577–3581.
5. **Burcham PC, Raso A, Thompson CA.** 2010. Toxicity of smoke extracts towards A549 lung cells: role of acrolein and suppression by carbonyl scavengers. Chem Biol Interact **183:**416–424. http://dx.doi.org/10.1016/j.cbi.2009.12.006.
6. **Feng Z, Hu W, Hu Y, Tang MS.** 2006. Acrolein is a major cigarette-related lung cancer agent: preferential binding at p53 mutational hotspots and inhibition of DNA repair. Proc Natl Acad Sci U S A **103:**15404–15409. http://dx.doi.org/10.1073/pnas.0607031103.
7. **Finkelstein EI, Nardini M, van der Vliet A.** 2001. Inhibition of neutrophil apoptosis by acrolein: a mechanism of tobacco-related lung disease? Am J Physiol Lung Cell Mol Physiol **281:**L732–L739.
8. **Dang TN, Arseneault M, Murthy V, Ramassamy C.** 2010. Potential role of acrolein in neurodegeneration and in Alzheimer's disease. Curr Mol Pharmacol **3:**66–78. http://dx.doi.org/10.2174/1874467211003020066.
9. **Huang YJ, Jin MH, Pi RB, Zhang JJ, Ouyang Y, Chao XJ, Chen MH, Liu PQ, Yu JC, Ramassamy C, Dou J, Chen XH, Jiang YM, Qin J.** 2013. Acrolein induces Alzheimer's disease-like pathologies in vitro and in vivo. Toxicol Lett **217:**184–191. http://dx.doi.org/10.1016/j.toxlet.2012.12.023.
10. **Singh M, Dang TN, Arseneault M, Ramassamy C.** 2010. Role of by-products of lipid oxidation in Alzheimer's disease brain: a focus on acrolein. J Alzheimers Dis **21:**741–756. http://dx.doi.org/10.3233/JAD-2010-100405.
11. **Aldini G, Orioli M, Carini M.** 2011. Protein modification by acrolein: relevance to pathological conditions and inhibition by aldehyde sequestering agents. Mol Nutr Food Res **55:**1301–1319. http://dx.doi.org/10.1002/mnfr.201100182.
12. **Tamamizu-Kato S, Wong JY, Jairam V, Uchida K, Raussens V, Kato H, Ruysschaert JM, Narayanaswami V.** 2007. Modification by acrolein, a component of tobacco smoke and age-related oxidative stress, mediates functional impairment of human apolipoprotein E. Biochemistry **46:**8392–8400. http://dx.doi.org/10.1021/bi700289k.
13. **Liu XY, Zhu MX, Xie JP.** 2010. Mutagenicity of acrolein and acrolein-induced DNA adducts. Toxicol Mech Methods **20:**36–44. http://dx.doi.org/10.3109/15376510903530845.
14. **Tang MS, Wang HT, Hu Y, Chen WS, Akao M, Feng Z, Hu W.** 2011. Acrolein induced DNA damage, mutagenicity and effect on DNA repair. Mol Nutr Food Res **55:**1291–1300. http://dx.doi.org/10.1002/mnfr.201100148.
15. **Wang HT, Hu Y, Tong D, Huang J, Gu L, Wu XR, Chung FL, Li GM, Tang MS.** 2012. Effect of carcinogenic acrolein on DNA repair and mutagenic susceptibility. J Biol Chem **287:**12379–12386. http://dx.doi.org/10.1074/jbc.M111.329623.
16. **Li H, Wang J, Kaphalia B, Ansari GA, Khan MF.** 2004. Quantitation of acrolein-protein adducts: potential biomarker of acrolein exposure. J Toxicol Environ Health A **67:**513–524. http://dx.doi.org/10.1080/15287390490276539.
17. **Wang HT, Zhang S, Hu Y, Tang MS.** 2009. Mutagenicity and sequence specificity of acrolein-DNA adducts. Chem Res Toxicol **22:**511–517. http://dx.doi.org/10.1021/tx800369y.
18. **Lee HW, Wang HT, Weng MW, Chin C, Huang W, Lepor H, Wu XR, Rom WN, Chen LC, Tang MS.** 2015. Cigarette side-stream smoke lung and bladder carcinogenesis: inducing mutagenic acrolein-DNA adducts, inhibiting DNA repair and enhancing anchorage-independent-growth cell transformation. Oncotarget **6:**33226–33236. http://dx.doi.org/10.18632/oncotarget.5429.
19. **Spiess PC, Deng B, Hondal RJ, Matthews DE, van der Vliet A.** 2011. Proteomic profiling of acrolein adducts in human lung epithelial cells. J Proteomics **74:**2380–2394. http://dx.doi.org/10.1016/j.jprot.2011.05.039.
20. **Lambert C, Li J, Jonscher K, Yang TC, Reigan P, Quintana M, Harvey J, Freed BM.** 2007. Acrolein inhibits cytokine gene expression by alkylating cysteine and arginine residues in the NF-kappaB1 DNA binding domain. J Biol Chem **282:**19666–19675. http://dx.doi.org/10.1074/jbc.M611527200.
21. **Moon KY.** 2011. Acrolein, an I-κBα-independent downregulator of NF-κB activity, causes the decrease in nitric oxide production in human

malignant keratinocytes. Arch Toxicol **85:**499–504. http://dx.doi.org/10.1007/s00204-010-0599-4.

22. **Mohammad MK, Avila D, Zhang J, Barve S, Arteel G, McClain C, Joshi-Barve S.** 2012. Acrolein cytotoxicity in hepatocytes involves endoplasmic reticulum stress, mitochondrial dysfunction and oxidative stress. Toxicol Appl Pharmacol **265:**73–82. http://dx.doi.org/10.1016/j.taap.2012.09.021.
23. **Chen D, Fang L, Li H, Tang MS, Jin C.** 2013. Cigarette smoke component acrolein modulates chromatin assembly by inhibiting histone acetylation. J Biol Chem **288:**21678–21687. http://dx.doi.org/10.1074/jbc.M113.476630.
24. **Burgess RJ, Zhang Z.** 2013. Histone chaperones in nucleosome assembly and human disease. Nat Struct Mol Biol **20:**14–22. http://dx.doi.org/10.1038/nsmb.2461.
25. **Fang L, Wuptra K, Chen D, Li H, Huang SK, Jin C, Yokoyama KK.** 2014. Environmental-stress-induced chromatin regulation and its heritability. J Carcinog Mutagen **5:**22058.
26. **Gurard-Levin ZA, Quivy JP, Almouzni G.** 2014. Histone chaperones: assisting histone traffic and nucleosome dynamics. Annu Rev Biochem **83:**487–517. http://dx.doi.org/10.1146/annurev-biochem-060713-035536.
27. **Ransom M, Dennehey BK, Tyler JK.** 2010. Chaperoning histones during DNA replication and repair. Cell **140:**183–195. http://dx.doi.org/10.1016/j.cell.2010.01.004.
28. **Adkins MW, Howar SR, Tyler JK.** 2004. Chromatin disassembly mediated by the histone chaperone Asf1 is essential for transcriptional activation of the yeast PHO5 and PHO8 genes. Mol Cell **14:**657–666. http://dx.doi.org/10.1016/j.molcel.2004.05.016.
29. **Groth A, Ray-Gallet D, Quivy JP, Lukas J, Bartek J, Almouzni G.** 2005. Human Asf1 regulates the flow of S phase histones during replicational stress. Mol Cell **17:**301–311. http://dx.doi.org/10.1016/j.molcel.2004.12.018.
30. **Jin C, Kato K, Chimura T, Yamasaki T, Nakade K, Murata T, Li H, Pan J, Zhao M, Sun K, Chiu R, Ito T, Nagata K, Horikoshi M, Yokoyama KK.** 2006. Regulation of histone acetylation and nucleosome assembly by transcription factor JDP2. Nat Struct Mol Biol **13:**331–338. http://dx.doi.org/10.1038/nsmb1063.
31. **Zhang H, Han J, Kang B, Burgess R, Zhang Z.** 2012. Human histone acetyltransferase 1 protein preferentially acetylates H4 histone molecules in H3.1-H4 over H3.3-H4. J Biol Chem **287:**6573–6581. http://dx.doi.org/10.1074/jbc.M111.312637.
32. **Ejlassi-Lassallette A, Mocquard E, Arnaud MC, Thiriet C.** 2011. H4 replication-dependent diacetylation and Hat1 promote S-phase chromatin assembly in vivo. Mol Biol Cell **22:**245–255. http://dx.doi.org/10.1091/mbc.E10-07-0633.
33. **Nagarajan P, Ge Z, Sirbu B, Doughty C, Agudelo Garcia PA, Schlederer M, Annunziato AT, Cortez D, Kenner L, Parthun MR.** 2013. Histone acetyl transferase 1 is essential for mammalian development, genome stability, and the processing of newly synthesized histones H3 and H4. PLoS Genet **9:**e1003518. http://dx.doi.org/10.1371/journal.pgen.1003518.
34. **Sobel RE, Cook RG, Perry CA, Annunziato AT, Allis CD.** 1995. Conservation of deposition-related acetylation sites in newly synthesized histones H3 and H4. Proc Natl Acad Sci U S A **92:**1237–1241. http://dx.doi.org/10.1073/pnas.92.4.1237.
35. **Parthun MR, Widom J, Gottschling DE.** 1996. The major cytoplasmic histone acetyltransferase in yeast: links to chromatin replication and histone metabolism. Cell **87:**85–94. http://dx.doi.org/10.1016/S0092-8674(00)81325-2.
36. **Campos EI, Fillingham J, Li G, Zheng H, Voigt P, Kuo WH, Seepany H, Gao Z, Day LA, Greenblatt JF, Reinberg D.** 2010. The program for processing newly synthesized histones H3.1 and H4. Nat Struct Mol Biol **17:**1343–1351. http://dx.doi.org/10.1038/nsmb.1911.
37. **Ejlassi-Lassallette A, Thiriet C.** 2012. Replication-coupled chromatin assembly of newly synthesized histones: distinct functions for the histone tail domains. Biochem Cell Biol **90:**14–21.
38. **Yang X, Yu W, Shi L, Sun L, Liang J, Yi X, Li Q, Zhang Y, Yang F, Han X, Zhang D, Yang J, Yao Z, Shang Y.** 2011. HAT4, a Golgi apparatus-anchored B-type histone acetyltransferase, acetylates free histone H4 and facilitates chromatin assembly. Mol Cell **44:**39–50. http://dx.doi.org/10.1016/j.molcel.2011.07.032.
39. **Burgess RJ, Zhou H, Han J, Zhang Z.** 2010. A role for Gcn5 in replication-coupled nucleosome assembly. Mol Cell **37:**469–480. http://dx.doi.org/10.1016/j.molcel.2010.01.020.
40. **Das C, Lucia MS, Hansen KC, Tyler JK.** 2009. CBP/p300-mediated acetylation of histone H3 on lysine 56. Nature **459:**113–117. http://dx.doi.org/10.1038/nature07861.
41. **Driscoll R, Hudson A, Jackson SP.** 2007. Yeast Rtt109 promotes genome stability by acetylating histone H3 on lysine 56. Science **315:**649–652. http://dx.doi.org/10.1126/science.1135862.
42. **Li Q, Zhou H, Wurtele H, Davies B, Horazdovsky B, Verreault A, Zhang Z.** 2008. Acetylation of histone H3 lysine 56 regulates replication-coupled nucleosome assembly. Cell **134:**244–255. http://dx.doi.org/10.1016/j.cell.2008.06.018.
43. **Chen CC, Carson JJ, Feser J, Tamburini B, Zabaronick S, Linger J, Tyler JK.** 2008. Acetylated lysine 56 on histone H3 drives chromatin assembly after repair and signals for the completion of repair. Cell **134:**231–243. http://dx.doi.org/10.1016/j.cell.2008.06.035.
44. **Verreault A, Kaufman PD, Kobayashi R, Stillman B.** 1998. Nucleosomal DNA regulates the core-histone-binding subunit of the human Hat1 acetyltransferase. Curr Biol **8:**96–108. http://dx.doi.org/10.1016/S0960-9822(98)70040-5.
45. **Hoek M, Stillman B.** 2003. Chromatin assembly factor 1 is essential and couples chromatin assembly to DNA replication in vivo. Proc Natl Acad Sci U S A **100:**12183–12188. http://dx.doi.org/10.1073/pnas.1635158100.
46. **Liu WH, Roemer SC, Port AM, Churchill ME.** 2012. CAF-1-induced oligomerization of histones H3/H4 and mutually exclusive interactions with Asf1 guide H3/H4 transitions among histone chaperones and DNA. Nucleic Acids Res **40:**11229–11239. http://dx.doi.org/10.1093/nar/gks906.
47. **Miller A, Chen J, Takasuka TE, Jacobi JL, Kaufman PD, Irudayaraj JM, Kirchmaier AL.** 2010. Proliferating cell nuclear antigen (PCNA) is required for cell cycle-regulated silent chromatin on replicated and nonreplicated genes. J Biol Chem **285:**35142–35154. http://dx.doi.org/10.1074/jbc.M110.166918.
48. **Moggs JG, Grandi P, Quivy JP, Jonsson ZO, Hubscher U, Becker PB, Almouzni G.** 2000. A CAF-1-PCNA-mediated chromatin assembly pathway triggered by sensing DNA damage. Mol Cell Biol **20:**1206–1218. http://dx.doi.org/10.1128/MCB.20.4.1206-1218.2000.
49. **Jin C, Felsenfeld G.** 2006. Distribution of histone H3.3 in hematopoietic cell lineages. Proc Natl Acad Sci U S A **103:**574–579. http://dx.doi.org/10.1073/pnas.0509974103.
50. **Fang L, Wang X, Yamoah K, Chen PL, Pan ZQ, Huang L.** 2008. Characterization of the human COP9 signalosome complex using affinity purification and mass spectrometry. J Proteome Res **7:**4914–4925. http://dx.doi.org/10.1021/pr800574c.
51. **Yu C, Kandur W, Kao A, Rychnovsky S, Huang L.** 2014. Developing new isotope-coded mass spectrometry-cleavable cross-linkers for elucidating protein structures. Anal Chem **86:**2099–2106. http://dx.doi.org/10.1021/ac403636b.
52. **Luger K, Rechsteiner TJ, Flaus AJ, Waye MM, Richmond TJ.** 1997. Characterization of nucleosome core particles containing histone proteins made in bacteria. J Mol Biol **272:**301–311. http://dx.doi.org/10.1006/jmbi.1997.1235.
53. **Luger K, Rechsteiner TJ, Richmond TJ.** 1999. Preparation of nucleosome core particle from recombinant histones. Methods Enzymol **304:**3–19. http://dx.doi.org/10.1016/S0076-6879(99)04003-3.
54. **Fang L, Jia KZ, Tang YL, Ma DY, Yu M, Hua ZC.** 2007. An improved strategy for high-level production of TEV protease in Escherichia coli and its purification and characterization. Protein Expr Purif **51:**102–109. http://dx.doi.org/10.1016/j.pep.2006.07.003.
55. **Kawase H, Okuwaki M, Miyaji M, Ohba R, Handa H, Ishimi Y, Fujii-Nakata T, Kikuchi A, Nagata K.** 1996. NAP-I is a functional homologue of TAF-I that is required for replication and transcription of the adenovirus genome in a chromatin-like structure. Genes Cells **1:**1045–1056. http://dx.doi.org/10.1046/j.1365-2443.1996.d01-223.x.
56. **Loyola A, LeRoy G, Wang YH, Reinberg D.** 2001. Reconstitution of recombinant chromatin establishes a requirement for histone-tail modifications during chromatin assembly and transcription. Genes Dev **15:**2837–2851.
57. **Eiserich JP, van der Vliet A, Handelman GJ, Halliwell B, Cross CE.** 1995. Dietary antioxidants and cigarette smoke-induced biomolecular damage: a complex interaction. Am J Clin Nutr **62:**1490S–1500S.
58. **Loyola A, Reinberg D.** 2003. Histone deposition and chromatin assembly by RSF. Methods **31:**96–103. http://dx.doi.org/10.1016/S1046-2023(03)00093-8.
59. **Loyola A, Huang JY, LeRoy G, Hu S, Wang YH, Donnelly RJ, Lane WS, Lee SC, Reinberg D.** 2003. Functional analysis of the subunits of the

chromatin assembly factor RSF. Mol Cell Biol **23:**6759–6768. http://dx.doi.org/10.1128/MCB.23.19.6759-6768.2003.

60. **Lu K, Boysen G, Gao L, Collins LB, Swenberg JA.** 2008. Formaldehyde-induced histone modifications in vitro. Chem Res Toxicol **21:**1586–1593. http://dx.doi.org/10.1021/tx8000576.
61. **Zhang J, Sprung R, Pei J, Tan X, Kim S, Zhu H, Liu CF, Grishin NV, Zhao Y.** 2009. Lysine acetylation is a highly abundant and evolutionarily conserved modification in Escherichia coli. Mol Cell Proteomics **8:**215–225. http://dx.doi.org/10.1074/mcp.M800187-MCP200.
62. **Wu J, Stevens JF, Maier CS.** 2011. Mass spectrometry-based quantification of myocardial protein adducts with acrolein in an in vivo model of oxidative stress. Mol Nutr Food Res **55:**1401–1410. http://dx.doi.org/10.1002/mnfr.201100255.
63. **Cai J, Bhatnagar A, Pierce WM, Jr.** 2009. Protein modification by acrolein: formation and stability of cysteine adducts. Chem Res Toxicol **22:**708–716. http://dx.doi.org/10.1021/tx800465m.
64. **Shao B, Fu X, McDonald TO, Green PS, Uchida K, O'Brien KD, Oram JF, Heinecke JW.** 2005. Acrolein impairs ATP binding cassette transporter A1-dependent cholesterol export from cells through site-specific modification of apolipoprotein A-I. J Biol Chem **280:**36386–36396. http://dx.doi.org/10.1074/jbc.M508169200.
65. **Stevens JF, Maier CS.** 2008. Acrolein: sources, metabolism, and biomolecular interactions relevant to human health and disease. Mol Nutr Food Res **52:**7–25. http://dx.doi.org/10.1002/mnfr.200700412.
66. **Shao B, O'Brien KD, McDonald TO, Fu X, Oram JF, Uchida K, Heinecke JW.** 2005. Acrolein modifies apolipoprotein A-I in the human artery wall. Ann N Y Acad Sci **1043:**396–403. http://dx.doi.org/10.1196/annals.1333.046.
67. **Diggle JH, McVittie JD, Peacocke AR.** 1975. The self-association of chicken-erythrocyte histones. Eur J Biochem **56:**173–182. http://dx.doi.org/10.1111/j.1432-1033.1975.tb02220.x.
68. **Zheng Y, Kim SH, Patel AB, Narayanaswami V, Iavarone AT, Hura GL, Bielicki JK.** 2012. The positional specificity of EXXK motifs within an amphipathic alpha-helix dictates preferential lysine modification by acrolein: implications for the design of high-density lipoprotein mimetic peptides. Biochemistry **51:**6400–6412. http://dx.doi.org/10.1021/bi300626g.